Electronic Supplementary Material (ESI) for Dalton Transactions.
This journal is © The Royal Society of Chemistry 2021

Supplementary SEM data

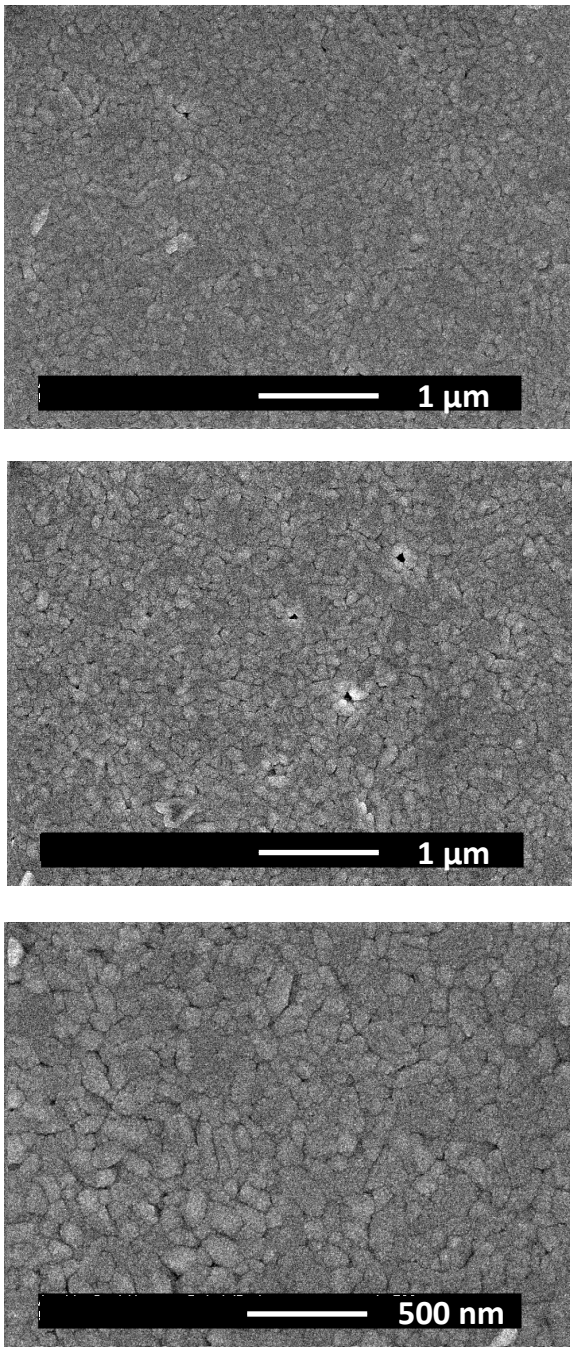

Fig. S1. Reduced magnification images for the Aurivillius $Bi_4Ti_{1.5}Mn_{0.5}Fe_{0.5}Nb_{0.5}O_{12}$ (x=0.5) ceramic processed by SPS of thermally treated powdered phases. Note the high microstructural homogeneity, consistently found all across the sample.

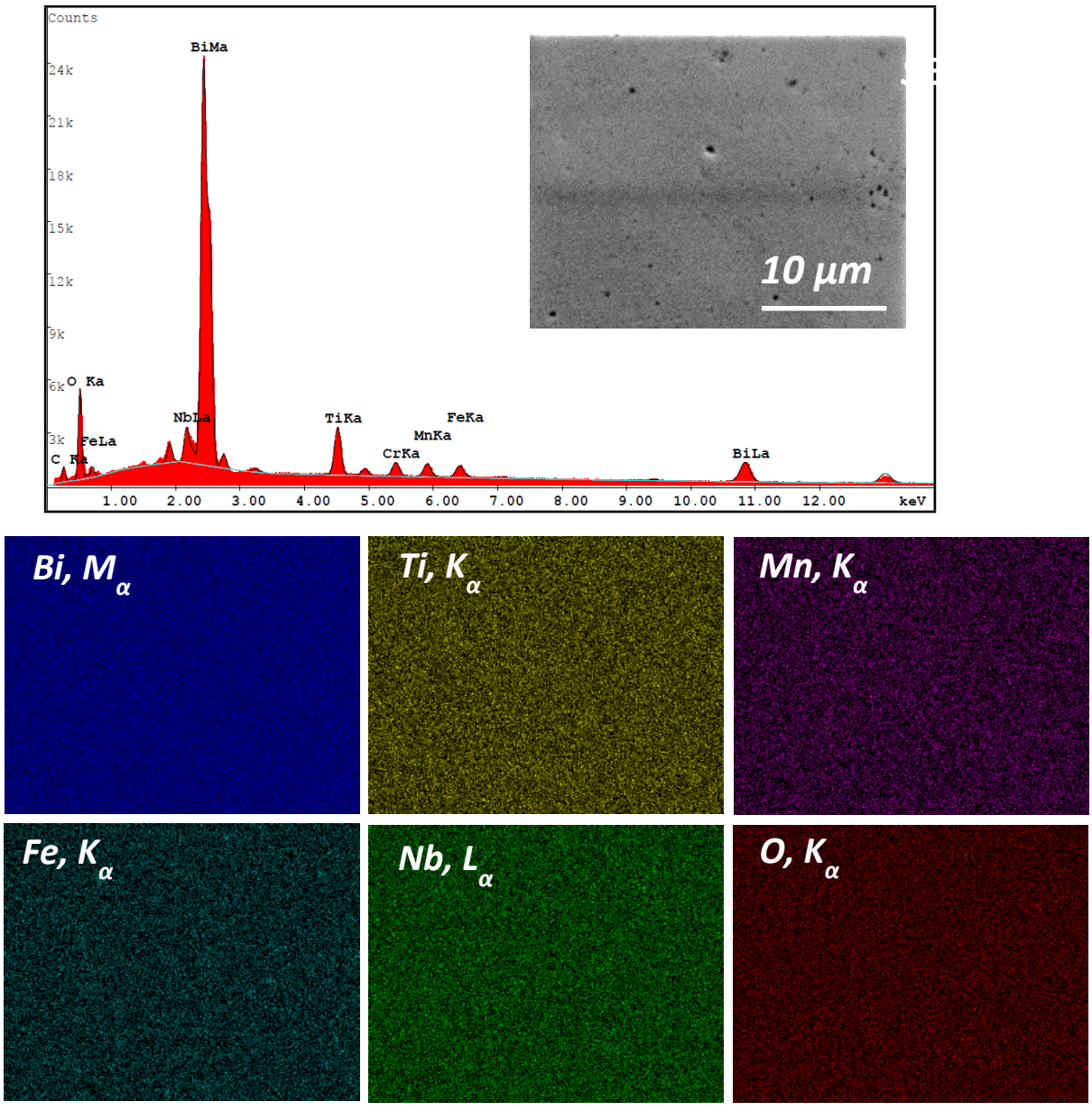

Fig. S2. EDXS accumulated spectrum and elementary mappings across a 30x25 µm^2 area for the $Bi_4Ti_{1.5}Mn_{0.5}Fe_{0.5}Nb_{0.5}O_{12}$ (x=0.5) ceramic material, where chemical heterogeneities are not observed. Cr signal originates from the conductive coating deposited to avoid charging effects.

Supplementary electrical data

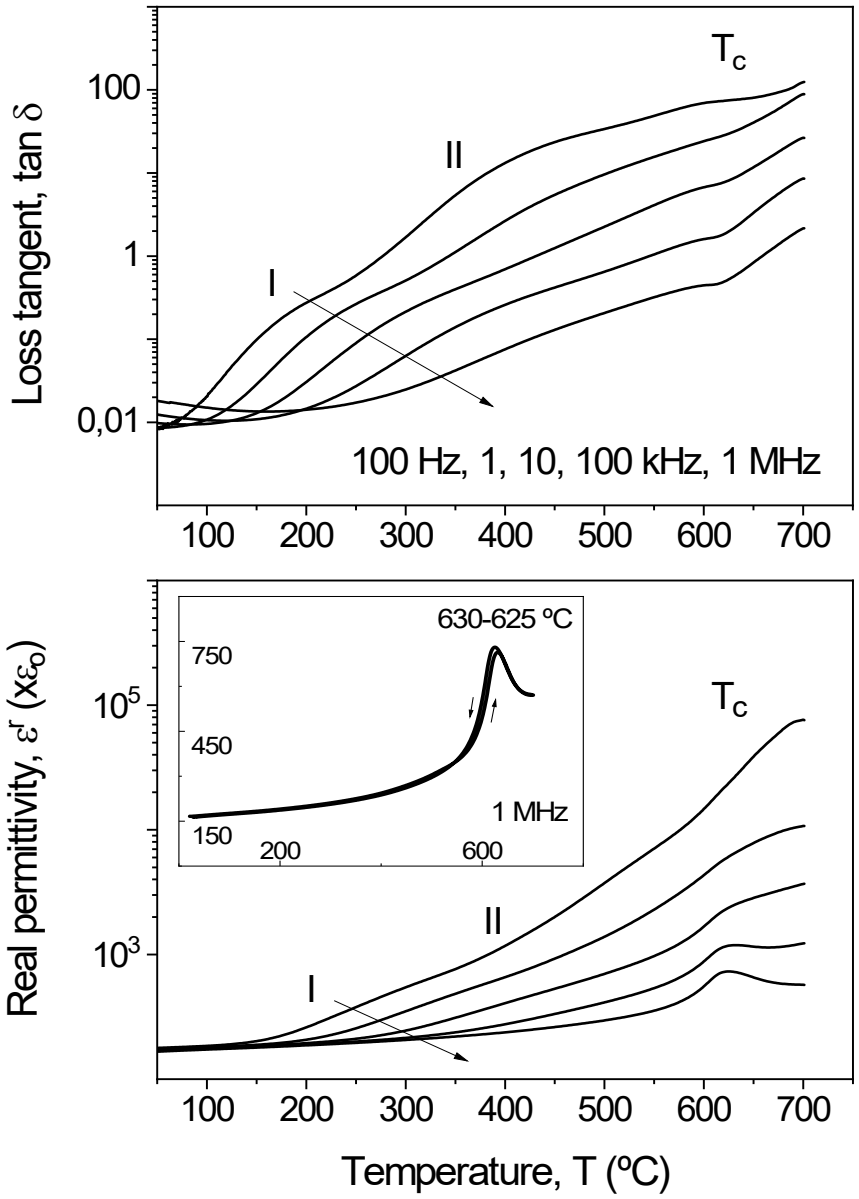

Fig. S3. Temperature dependences of the dielectric permittivity (bottom) and losses (top) for the $Bi_4Ti_2Nb_{0.5}Fe_{0.5}O_{12}$ (x=0) ceramic processed by SPS, at several frequencies. The two successive dielectric relaxations and the ferroelectric transition are labelled as I, II and T_C. Inset shows the thermal

hysteresis across the transition anomaly at 1 MHz (Curie temperatures are indicated).

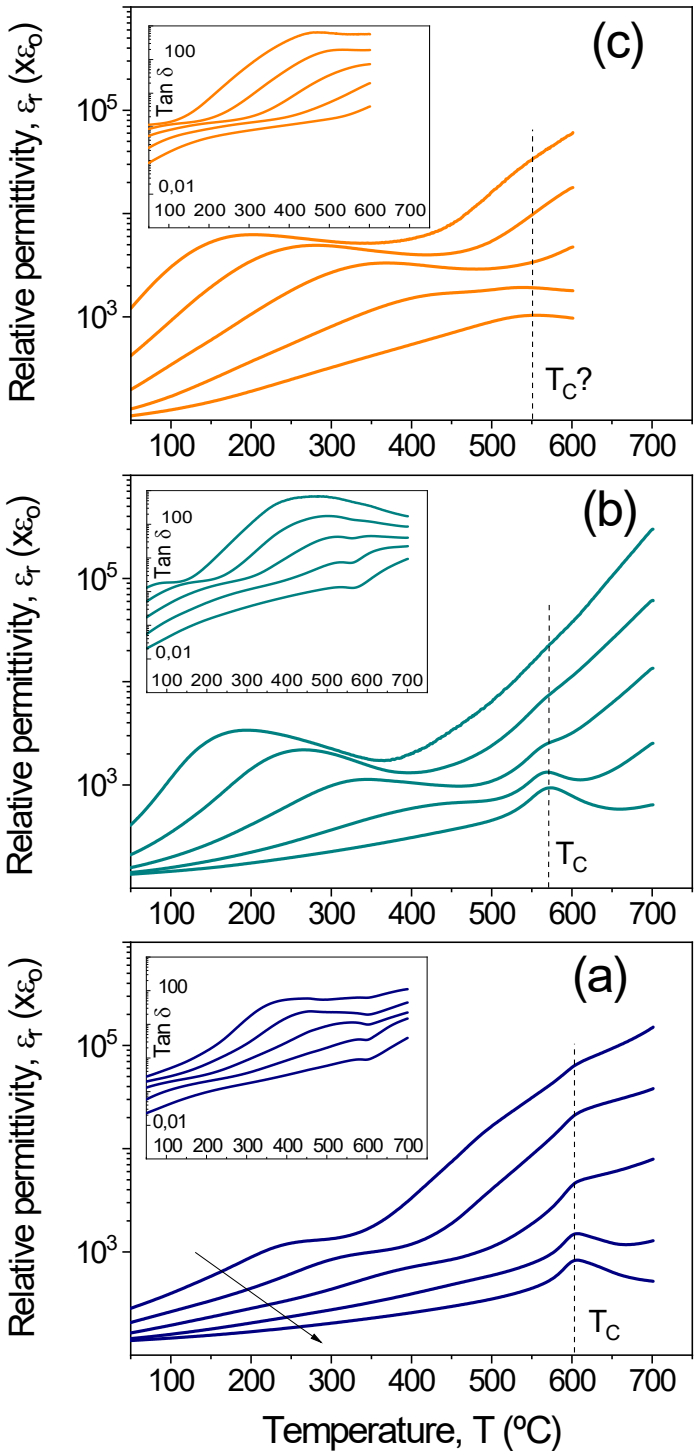

Fig. S4. Temperature dependence of the dielectric permittivity for the $Bi_4Ti_{2-x}Mn_xFe_{0.5}Nb_{0.5}O_{12}$ ceramic materials with (a) x=0.1, (b) x=0.3, and (c) x= 0.5, at five frequencies (100 Hz, 1, 10 and 100 kHz, and 1 MHz; arrow indicates

increasing f). Note the Maxwell-Type type relaxation at intermediate temperatures, and the ferroelectric transition above it marked with T_C. Insets show corresponding loss tangent.

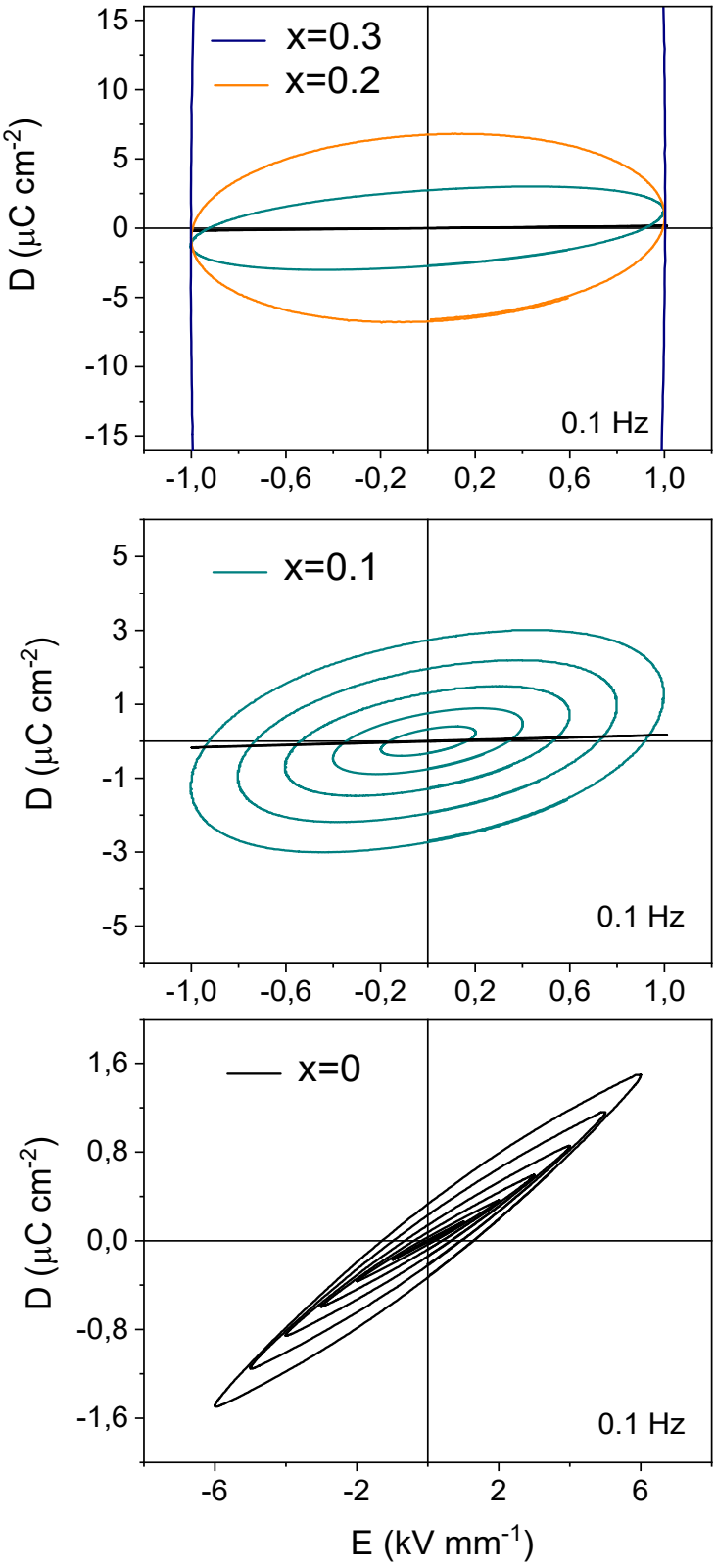

Fig. S5. RT high field electrical response for the $Bi_4Ti_{2-x}Mn_xFe_{0.5}Nb_{0.5}O_{12}$ ceramic materials. Note the Rayleigh-type behaviour for x=0, and the increasing leakage currents with x.

Supplementary PFM data

Fig. S6. (a) Topography, and piezoresponse (b) amplitude and (c) phase images of $Bi_4Ti_2Mn_{0.5}Fe_{0.5}Nb_{0.5}O_{12}$ (x=0.5) demonstrating the presence of ferroelectric inversion domains.

Supplementary magnetic data

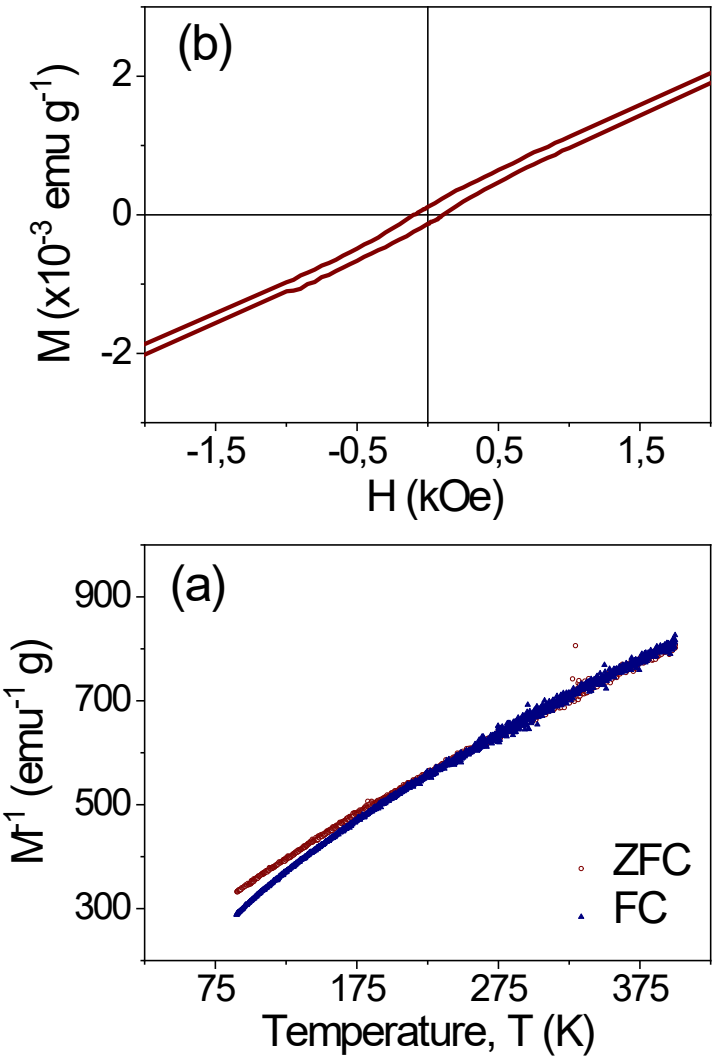

Fig. S7. (a) ZFC and FC reciprocal magnetizations at 300 Oe and increasing temperatures for the $Bi_4Ti_{1.8}Mn_{0.2}Fe_{0.5}Nb_{0.5}O_{12}$ (x=0.2) ceramic material, and (b) isothermal magnetization for the same Aurivillius phase at 100 K (the paramagnetic high field linear contribution has been substracted). Note the appearance of irreversibility at low temperature, and the presence of hysteresis in the high field response.